JOURNAL

OF THE AMERICAN CHEMICAL SOCIETY

VOLUME 108, NUMBER 2 JANUARY 22, 1986

Monte Carlo Simulation Studies of the Solvation of Ions. 1. Acetate Anion and Methylammonium Cation

Giuliano Alagona,† Caterina Ghio,† and Peter Kollman*

Contribution from the Istituto di Chimica Quantistica ed Energetica Molecolare del CNR, I-56100 Pisa, Italy, and Department of Pharmaceutical Chemistry, School of Pharmacy, University of California, San Francisco, California 94143. *Received January 31, 1985*

Abstract: Monte Carlo (MC) simulations have been carried out on acetate anion (CH_3COO^-) and methylammonium cation ($CH_3NH_3^+$), in water, using the TIP4P potential for water and analogous potentials for the ions. Analysis of the water structure around the two ions suggests four types of water: (1) those tightly bound to the $O^{\delta-}$ of the acetate, (2) those tightly bound to the $H^{\delta+}$ of the methylammonium, (3) hydrophobically bound waters near the CH_3 groups, and (4) bulk waters. Enthalpies of solvation of −80 and −66 kcal/mol are calculated for acetate and methylammonium, respectively, both in reasonable agreement with experimental values. The nature of the water structure around the methyl group of $CH_3NH_3^+$ is significantly different from that around both CH_3COO^- and $(CH_3O)_2PO_2^-$, which may have important implications in the nature of molecular interactions of protonated amines.

Protein–ligand interactions involve hydrophobic, hydrogen-bonding, and ionic interactions. In one of the best characterized of such interactions, the interaction free energies of thyroxine analogues with prealbumin have been shown to be very dependent on the nature of the side chain, with the analogue with a COO^- side chain binding about 1000 times more strongly than the analogue with the NH_3^+ side chain.[1] We have been able to *qualitatively* reproduce this difference with molecular mechanical calculations[2] but showed, in general, that differential solvation effects were important in understanding relative binding energies of thyroxine analogues to prealbumin.

Protonated amines are an essential functional group in almost all neurotransmitters and in a large number of other molecules of biological importance.[3] Given the importance of NH_3^+ and COO^- groups in molecules of biological interest and the role of solvation by water in influencing the interactions of these groups with other functional groups and each other, we have initiated a study of the solvation of these groups, using $CH_3NH_3^+$ and CH_3COO^- as models.

Methods

The simulations have been carried out at 25 °C and 1 atm in the NPT ensemble, using periodic boundary conditions and preferential sampling, with a nonbonded cutoff of 8.5 Å, on the Gould 32/8705 at ICQEM, Pisa.

We began both simulations starting from an arbitrary configuration of 216 pure water molecules placed around a bulkier solute. Rigid moves of the solute were allowed throughout all the equilibration every 500 steps, unless otherwise stated. We raised the temperature to 1000 °C and maintained it at that value for 100K steps at constant volume (V = 6617.5 Å^3) before lowering the temperature to the desired value of 25 °C.

Table I. Parameters Employed in the MC Simulations[a]

	atom type	$A^2 \times 10^{-3}$	C^2	q
H_2O-TIP4P[b]	O	600	610	0
	M[c]	0	0	−1.04
	H	0	0	0.52
CH_3COO^-[d]	CH_3	7950	2400	−0.208
	C	789.954	615.77	0.620
	O2	230.584	429.5	−0.706
$CH_3NH_3^+$[d]	CH_3	7950	2400	0.338
	N	990.525	563	−0.274
	H	0	0	0.312

[a] Units: electrons for q, kcal Å^{12}/mol for A^2, kcal Å^6/mol for C^2. [b] Experimental geometry (R(O–H) = 0.9572 Å, ∠HOH = 104.52°), parameters from ref 9. [c] M is a point between the H's along the bisector of HOH angle, 0.15 Å from oxygen. [d] Charges obtained from the best fit to the electrostatic potential[17] produced by a 6-31G* basis set. CH_3 values are TIPS parameters for CH_3;[18] O2, C, H, and N parameters are taken from ref 6, except for the hydrogen-bonding H Lennard-Jones parameter, which was set equal to 0 to be consistent with the H in TIP4P. Geometry taken from standard geometries in ref 6, with R(C–N) = 1.47 Å in $CH_3NH_3^+$, R(N–H) = 1.0 Å, a tetrahedral coordination around N, R(C–C) = 1.51 Å, R(C–O) = 1.25 Å, and ∠OCO = 126° in the acetate ion.

During the next 200K steps the volume was allowed to change by 100 Å^3 at most, every 5000 steps. Then we raised the frequency of solute moves up to once every 200 MC steps for a total of 300K steps, during which the volume moves reached the frequency of once every 500 steps.

* Address correspondence to University of California.
† Istituto di Chimica Quantistica ed Energetica Molecolare del CNR.

(1) Andrea, T. A.; Cavalieri, R. R.; Goldfine, I. D.; Jorgensen, E. C. *Biochemistry* **1980**, *19*, 55.
(2) Blaney, J. M.; Weiner, P. K.; Dearing, A.; Kollman, P. A.; Jorgensen, E. C.; Oatley, S. J.; Burridge, J. M.; Blake, C. C. F. *J. Am. Chem. Soc.* **1982**, *104*, 6424.
(3) Wolff, M. Ed., In "The Basis of Medicinal Chemistry", Burger's Medicinal Chemistry, 4th ed., Wiley: New York, 1979.

0002-7863/86/1508-0185$01.50/0

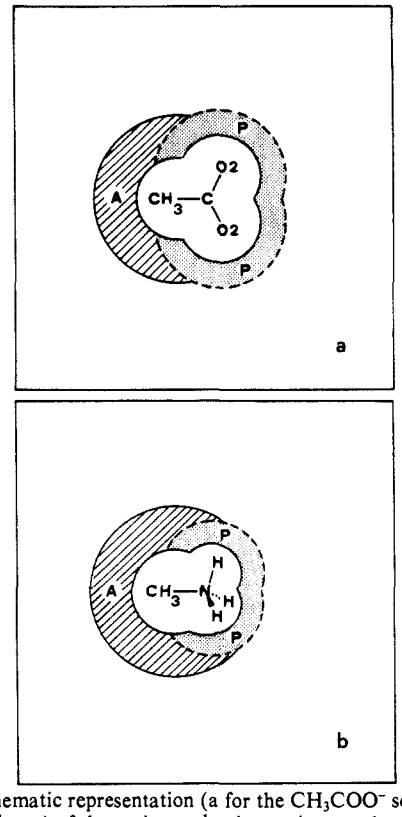

Figure 1. Schematic representation (a for the CH_3COO^- solution, b for the $CH_3NH_3^+$ one) of the various solvation regions: polar, P; nonpolar, A; bulk, all the rest. The blank area immediately surrounding the solute corresponds to its excluded volume.

Finally, we allowed the systems to equilibrate for 900K steps. We determined averages by using the next 2100K steps for the $CH_3NH_3^+$ simulation and 2500K[4] steps for the CH_3COO^- one.

Although one cannot rule out that the system is trapped in a local minimum and much longer simulations might be required to ensure a complete representation of solvation space, the radial distribution and energy properties are well converged after ~2000K steps.

The intermolecular potential between monomer m and n (of the type 12-6-1) employed in the simulations is

$$\epsilon_{mn} = \sum_i^{onm} \sum_j^{onn} \left(\frac{q_i q_j e^2}{r_{ij}} + \frac{A_i A_j}{r_{ij}^{12}} - \frac{C_i C_j}{r_{ij}^{6}} \right) \quad (1)$$

The Coulombic and Lennard-Jones parameters for the two ions and for water are reported in Table I. We have used Jorgensen's TIPS parameters where available. The $O^{\delta-}$ parameters (O2) have been used in previous simulations on dimethyl phosphate (DMP),[5] where they were satisfactory. For the other atoms, we have employed the van der Waals parameters previously derived.[6]

In order to analyze the solvation of the acetate anion and the methylammonium cation, we focus on their two different solvation sites, (A) hydrophobic (CH_3) and (P) polar ($O^{\delta-}$ and $H^{\delta+}$), that are much closer to each other than the corresponding zones in DMP. This produces some ambiguity in the definition of the different zones. Parts a and b of Figure 1 illustrate the geometrical definition of the various zones we have used for CH_3COO^- and $CH_3NH_3^+$, respectively. In the ensuing analyses, we will see that no waters are found in the zone between the A and P regions; therefore, there is no ambiguity in assigning waters to the A and P zones.

Results

Solute–Solvent Structural Analysis. We report in Figure 2 and in Figure 3, for acetate and methylammonium respectively, the radial distribution functions (rdf's) for the methyl groups and the

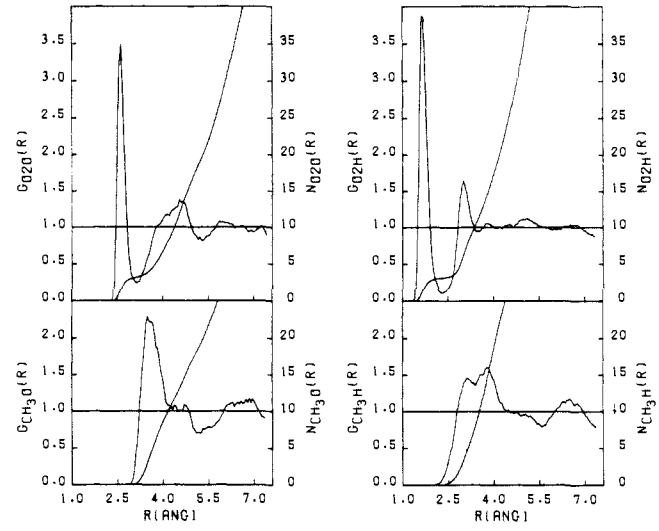

Figure 2. Radial distribution functions (left scales) and running coordination numbers (right scales) between the solute groups and water O (left) and H (right) in the acetate solution: $g_{CH_3O}(r)$, $g_{CH_3H}(r)$, $N_{CH_3O}(r)$, $N_{CH_3H}(r)$ (lower) and $g_{OO}(r)$, $g_{OH}(r)$, $N_{OO}(r)$, $N_{OH}(r)$ (upper).

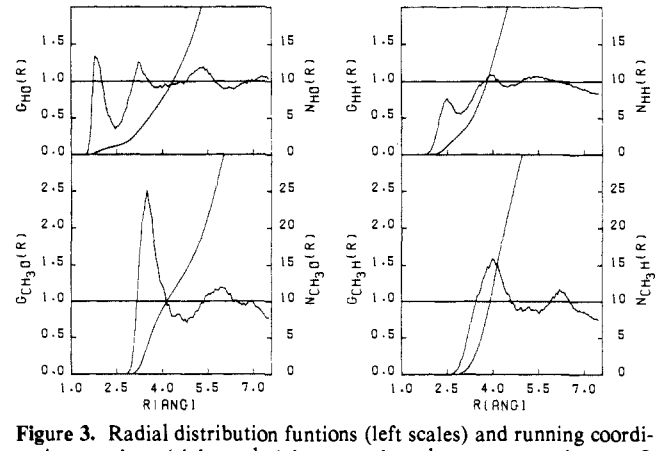

Figure 3. Radial distribution funtions (left scales) and running coordination numbers (right scales) between the solute groups and water O (left) and H (right) in the methylammonium solution: $g_{CH_3O}(r)$, $g_{CH_3H}(r)$, $N_{CH_3O}(r)$, $N_{CH_3H}(r)$ (lower) and $g_{HO}(r)$, $g_{HH}(r)$, $N_{HO}(r)$, $N_{HH}(r)$ (upper).

average radial distribution functions for the polar groups, together with the running coordination numbers. We do not consider the rdf's for the inner group (C of the carboxylate ion and N of the ammonium), because their short range trend is analogous to that of the polar part of the molecule, just shifted by an amount equal to the N–H or the C–O distance. The radial distribution functions have been recorded every step, scanning the space surrounding the molecule with a Δr = 0.055 Å.

In the rdf's of the hydrophobic group (g_{CH_3O}) for both ions, the first peak occurs at nearly 3.7 Å in both cases. The shape of the CH_3O rdf's is similar to that found, for instance, in alanyldipeptide,[7] ethanol,[8] and DMP[5] and is close to what was previously found also for spherical solutes. In the $CH_3NH_3^+$ solution, the shape of the first peak is similar to that of spherical solutes because of the presence of the waters coordinated to the N–H's, the O of which lies within the first-shell solvation radius of CH_3. In the acetate solution, the water oxygens coordinated to the anionic oxygens are farther from the methyl group, leading to a different shape of g_{CH_3H} in the two ions. In the $CH_3NH_3^+$ solution, we have a broad peak, with the center at about 4 Å, including the H's of the waters coordinated by the ammonium group hydrogens. In the CH_3COO^- solution, we have two distinct peaks, one shorter

(4) Initially, we averaged both solutions over 2100K steps, a small difference between the rdf's of the two acetate oxygens caused us to continue the simulation for 400K more steps, but no substantial change occurred.

(5) Alagona, G.; Ghio, C.; Kollman, P. *J. Am. Chem. Soc.* **1985**, *107*, 2229.
(6) Weiner, S. J.; Kollman, P. A.; Case, D. A.; Singh, U. C.; Ghio, C.; Alagona, G.; Profeta, S.; Weiner, P. *J. Am. Chem. Soc.* **1984**, *106*, 765.
(7) Rossky, P. J.; Karplus, M. *J. Am. Chem. Soc.* **1979**, *101*, 1913.
(8) Alagona, G.; Tani, A. *Chem. Phys. Lett.* **1982**, *87*, 337.
(9) Jorgensen, W. L.; Chandrasekhar, J.; Madura, J. D.; Impey, R. W.; Klein, M. L. *J. Chem. Phys.* **1983**, *79*, 926.

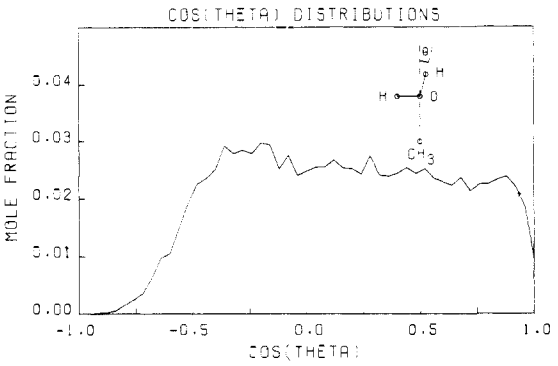

Figure 4. Cos θ distributions for the waters belonging to the CH_3 region in the methylammonium solution. θ angle defined as depicted. Units for the ordinate are mole fraction/0.04 cos θ.

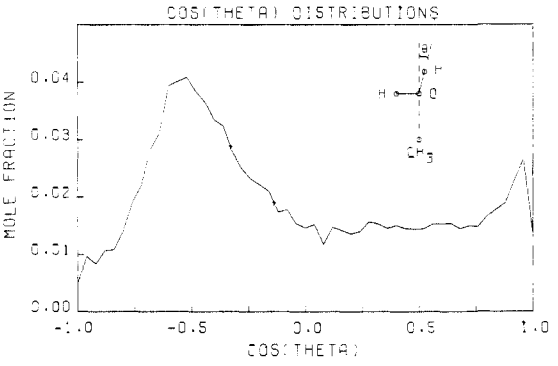

Figure 5. Cos θ distributions for the waters belonging to the CH_3 region in the acetate solution. θ angle defined as depicted. Units for the ordinate are mole fraction/0.04 cos θ.

at about 3.1 Å, likely due to the H's of CH_3 coordination waters, and the other at about 3.8 Å, due to the waters coordinated by the O2's.

In these simulations, the CH_3 groups are not completely electroneutral; in particular, the methyl group in $CH_3NH_3^+$ has a significant positive partial charge that orients the waters so that their H's are farther from the methyl group than in acetate, as can be seen both from the CH_3H rdf and from the cos θ distributions displayed in Fgures 4 and 5. The angle θ is defined, as depicted, as the angle formed by the O–H direction with the axis CH_3–O directed outward. Almost no H is directed toward the CH_3 within a cone for $180° > \theta > 140°$, while almost all the hydrogens are within a solid angle $120° > \theta > 0°$ with equal probability. Thus, it is likely that one or both O lone pairs point toward the CH_3. In contrast, the methyl group in CH_3COO^-, even though it bears a partial charge double in magnitude and of opposite sign of that of a DMP CH_3, behaves analogously to the methyl groups in DMP.[5] Figure 5 makes clear that configurations with hydrogens or lone pairs pointing toward the methyl group are disfavored.

The g_{OO} and g_{OH} rdf's for the acetate O2 are analogous to those for DMP. As previously, we have a strong H bond between the O2's and three waters, each of which is pointing one of its H's toward O2. The orientation of the waters coordinated to O2 is made clear by the cos θ distribution (Figure 6), which shows two equivalent peaks at 180° and 75.5°, exactly consistent with the H–O–H bond angle of H_2O (104.5°).

In the $CH_3NH_3^+$ cation, the waters are strongly oriented with both O lone pairs toward the NH_3^+ H's, as can be seen both from the fact that the running coordination number for g_{HH} increases twice as fast as that for g_{HO}, starting half a water OH bond length farther apart, and from the cos θ distribution (Figure 7). Note the difference between this distribution and that around CH_3 (Figure 4), where there is a tendency to have a lone pair directed toward CH_3 but no preferred orientation.

Another distinctively different feature of the two polar regions is made clear by the differential distance distributions.[5] While

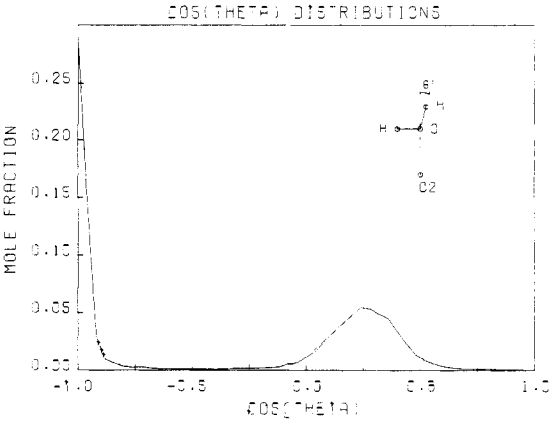

Figure 6. Cos θ distributions for the waters belonging to the polar O2 region in the acetate solution. θ angle defined as depicted. Units for the ordinate are mole fraction/0.04 cos θ.

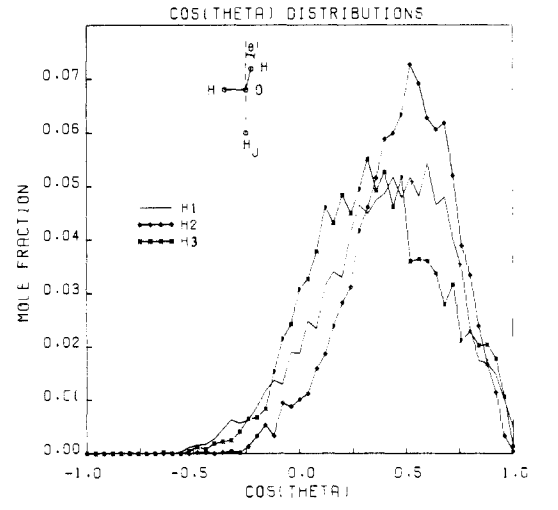

Figure 7. Cos θ distributions for the waters belonging to the polar H in the methylammonium solution. θ angle defined as depicted. Units for the ordinate are mole fraction/0.04 cos θ.

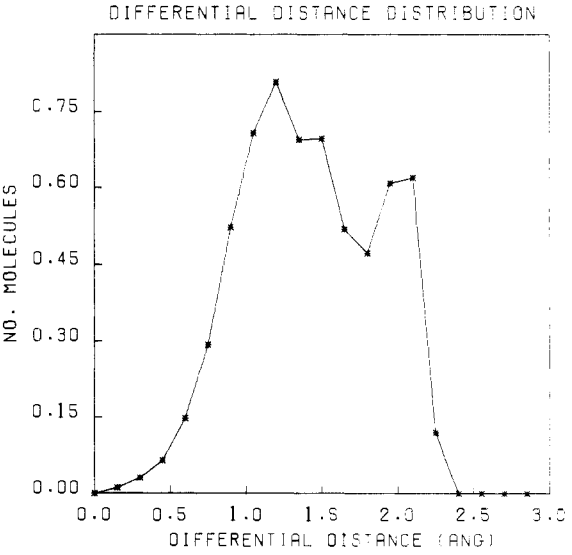

Figure 8. Differential O2–O distance distributions for the waters belonging to the polar O2 region in the acetate solution. Units for the ordinate are no. of molecules/0.15 Å.

no O is bridged between the two O2 oxygens (Figure 8), a fairly large number of water oxygens are bridged between two different H's of the NH_3^+ group (Figure 9), and this results in a coordination number slightly larger than 1 for these H's. This distribution shows a distinct peak at around 1.5 Å, corresponding to

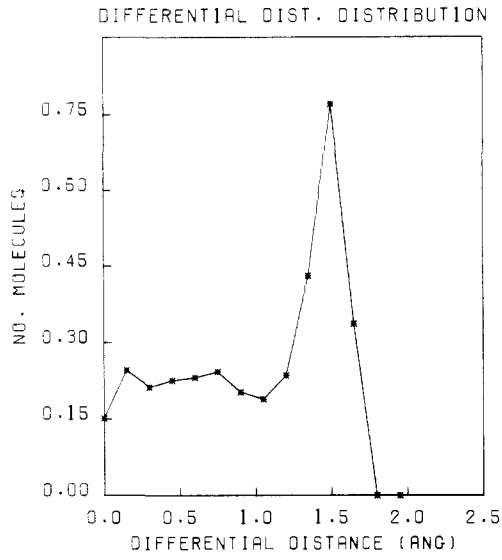

Figure 9. Differential H–O distance distributions for the waters belonging to the polar H region in the methylammonium solution. Units for the ordinate are no. of molecules/0.15 Å.

the highly ordered structure in which a water molecule is associated with each ammonium H,

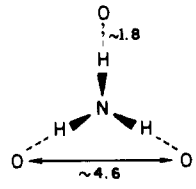

at a distance of 1.8–1.9 Å along the N–H direction. In this way, the water oxygens are kept at a distance of about 4.6 Å from each other. Since they are so far apart, it is not unreasonable that another water molecule inserts itself in between, which is the origin of the calculated NH_3^+ coordination number of ~3.5.

A further analysis of the differential distance distribution around the O2 is also interesting. Given an average distance between a water O and the closest O2 of 2.7 Å, the differential distance distribution corresponds to angular values in the range 96°–150° (with a slightly lower population about 132°) and is consistent with an almost tetrahedral position around each C–O axis of three freely rotating waters. This is somewhat different than the situation around the DMP O2's, where we have been able to distinguish between staggered and eclipsed arrangements. This difference is likely due to the fact that, in DMP, there are other functional groups (OCH_3) restricting the allowed coordination around the POO^- group.

Solute–Solvent Energy Analysis. Assuming pairwise additivity, the total potential energy of the solution can be written as

$$E = \sum_{i=1}^{N} E_{S_iX} + \sum_{i=1}^{N}\sum_{j>i}^{N} E_{S_iS_j} = \bar{E}_{SX} + E_{SS} \qquad (2)$$

The partial molar internal energy $\Delta\bar{E}_{soln}$ (or energy of solution) is

$$\Delta\bar{E}_{soln} = \bar{E}_{SX} + E_{SS} - E_{SS}^{\circ} = \bar{E}_{SX} + \Delta\bar{E}_{SS} \qquad (3)$$

where, E_{SS}° being the total energy of an equal number of pure water molecules, $\Delta\bar{E}_{SS}$ can be considered as the solvent reorganization energy induced by the presence of the solute. The partial molar volume is defined analogously

$$\Delta\bar{V}_{soln} = V - V^{\circ} \qquad (4)$$

The bar indicates all the partial molar quantities. At 1 atm, since $P\Delta V_{soln} \approx 0$, the enthalpy of solution is

$$\Delta\bar{H}_{soln} \approx \Delta\bar{E}_{soln} - RT \qquad (5)$$

where RT is the PV contribution for the solute in the ideal gas.

Table II. Calculated Properties for CH_3COO^- and $CH_3NH_3^+$ at 1 atm and 25 °C[a]

property[b]	CH_3COO^-	$CH_3NH_3^+$
E	−2261.3 ± 2.1	−2247.7 ± 2.8
$\bar{E}_{SX}$	−152.6 ± 0.7	−133.4 ± 0.7
E_{SS}[c]	−2108.7 ± 2.2	−2114.3 ± 2.9
$\Delta\bar{E}_{SS}$	73.50 ± 4.1[d]	67.9 ± 4.5[d]
$\Delta\bar{E}_{soln}$	−79.1 ± 4.2[d]	−65.5 ± 4.6[d]
V°	6534.3 ± 9.2	6512.8 ± 9.4
$\Delta\bar{V}_{soln}$	53.8 ± 18.9[d]	40.8 ± 18.9[d]
$\Delta\bar{H}_{soln}$	−79.6 ± 4[d]	−66.0 ± 5[d]
ρ^{c}	1.0039	1.0003

[a] Energies are in kcal/mol; V is in Å^3, $\Delta\bar{V}_{soln}$ is in cm^3/mol; ρ is in g/cm^3. [b] As defined in text (eq 2–5). [c] Pure water TIP4P values[19] E_{SS}° = −2182.2 ± 3.4, V° = 6445 ± 30, ρ° = 1. [d] The standard deviations of the calculated difference quantities are the square roots of the sums of the component variances.

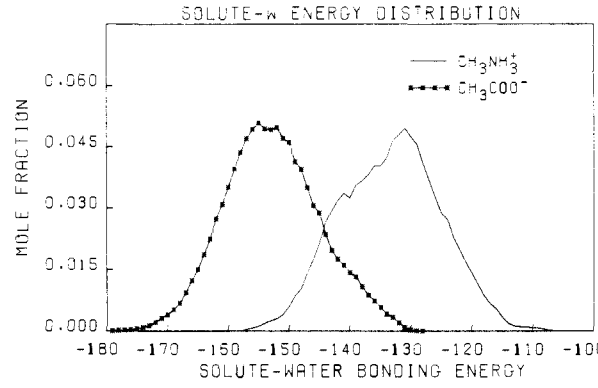

Figure 10. Solute–water energy distributions for CH_3COO^- and for $CH_3NH_3^+$. Units for the ordinate are mole fraction/kcal/mol.

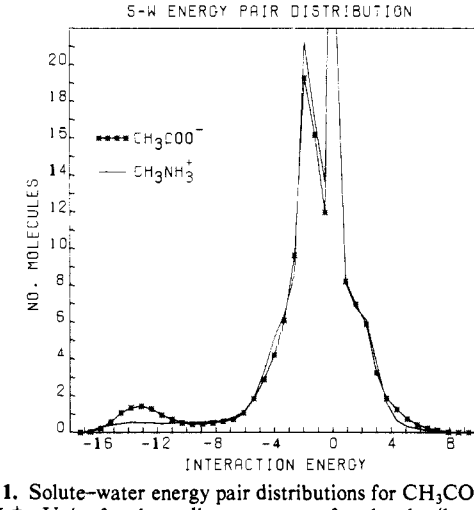

Figure 11. Solute–water energy pair distributions for CH_3COO^- and for $CH_3NH_3^+$. Units for the ordinate are no. of molecules/kcal/mol.

The computed results for these properties are reported in Table II. The acetate anion has a more favorable solvation energy by nearly 13.5 kcal/mol due to a better solute–solvent interaction (~19 kcal/mol) that, as usual, produces a larger total disruption (by 5.5 kcal/mol) in the solvent. However, the solvent reorganization energy is not as large a percentage of the solute–solvent interaction energy as in the DMP simulation.[5]

The calculated solvation enthalpies for acetate (−80 kcal/mol) and methylammonium (−66 kcal/mol) can be compared with the experimental values of −90[10] and −75 kcal/mol,[11] respectively.

(10) Calculated by using a thermodynamic cycle with $H_f(CH_3COOH,g)$, $H_f(CH_3COOH,aq)$, $H_f(CH_3COO^-,aq)$, and $H_f(H^+,aq)$ taken from: Wagman, D. "Selected Values of Thermodynamic Properties"; U.S. Government Printing Office: Washington, DC, 1968, and the proton affinity (ΔH for $CH_3COOH(g) \rightarrow CH_3COO^-(g) + H^+$) taken from: Kebarle, P. In "Environmental Effects on Molecular Structure and Properties"; Pullman, Reidel: Dordrecht, Holland, 1976; pp 81–93.

Table III. Decomposition of the Solvent–Solute (S–X) Interaction Energy within the First Shell[a]

	CH_3COO^-	$CH_3NH_3^+$	$\langle E\rangle_-$	$\langle E\rangle_+$	N_-	N_+
E'_{SXP}	−78.98	−42.25	−12.50	−12.17	6.32	3.47
E'_{SXA}	−9.09	−20.33	−1.45	−3.04	6.29	6.69
E'_{SX1}[b]	−88.07	−62.58			12.61	10.16
E'_{SXE}[c]	−64.53	−70.81	−0.88[d]	−0.93[d]	73.4	75.8
			(−0.32)	(−0.34)	203.4	205.8
E_{SX}[e]	−152.60	−133.40			216	216

[a] Energies are in kcal/mol; N is the number of water molecules in each zone. [b] The solvent–solute interaction energy with the water molecules in the first shell (E'_{SX1}) has been decomposed to E'_{SXP} and E'_{SXA}, where SXP and SXA indicate the contributions due to waters belonging to the polar P and apolar A regions; 2 Å ≤ R ≤ 3.2 Å around O2, 1.5 Å ≤ R ≤ 2.5 Å around H, and 2 Å ≤ R ≤ 4.2 Å around CH_3. [c] E'_{SXE} is the interaction energy between solute and waters external to the first shell. [d] Average with the exclusion of water molecules (~130) having 0 kcal/mol interaction energy with the solute. In parentheses the total average is reported. [e] E_{SX} is the overall solvent–solute interaction energy.

Both solvation enthalpies are underestimated by ~10% in magnitude, but the relative values seem well reproduced.

The partial molar volumes are 54 and 41 cm³/mol for acetate and methylammonium, respectively, in good agreement with the experimental values[12] (40.46 cm³/mol for acetate and 36.11 cm³/mol for methylammonium).

Figure 10 contains the solute–solvent energy distributions, which are smoother for acetate than methylammonium, perhaps because of the somewhat greater length of the simulation carried out for the anion. Both energy distributions have almost equal standard deviation, despite the difference in the average values.

The solute–solvent energy pair distributions (Figure 11) record the individual solute–solvent interaction energies. The largest difference in the distributions is found in the most attractive region; this can be attributed to the polar interactions, which integrate to 3.57 molecules for the methylammonium ion and 6.05 for acetate with interaction energies −20 < E < −9.6 kcal/mol. These coordination numbers are consistent with the coordination numbers of O2 and H (Table III).

The shape of the solute–solvent energy pair distribution of the acetate is quite similar to the DMP one;[5] only the hump at ~−13 kcal/mol is more pronounced and shifted toward more attractive energies for CH_3COO^-, due to the larger negative charges on the oxygens. The distributions are quite similar in the region above −8 kcal/mol, where the main differences arise from the slightly larger number of water molecules (42 vs. 40) having interaction energies with the solute in the weakly attractive range −2.5 < E < −0.5 kcal/mol around $CH_3NH_3^+$ and the slightly fewer number of waters in the $CH_3NH_3^+$ solution (1 vs. 2) having interaction energies E > 4 kcal/mol. These two differences can be attributed to the more attractive water interactions with the apolar region of $CH_3NH_3^+$ and to the larger number of waters in the polar region in acetate. In acetate, second-shell waters which are H-bonded to the first-shell ones may assume unfavorable positions with respect to the solute.

In Table III, in addition to the coordination numbers inside the various regions, the decomposition of the position dependent solute–solvent interaction energy is presented, together with the average contribution due to each type of coordinated water. The space surrounding the solute has been divided according to Figure 1 (a,b), considering the waters lying within a radius of 2–3.2 Å from each O2 or of 1.5–2.5 Å from each H as belonging to the polar shell and those within a radius of 2–4.2 Å from the methyl group (excluding the molecules already taken into account) as belonging to the apolar shell. All the other water molecules are considered to be in the bulk solution.

On average, there is a slightly stronger water–solute interaction with the polar O2 compared to the polar H, while the average interaction of waters with the methyl group is more favorable in the cation. The interaction with the external waters is slightly worse for CH_3COO^-, whereas on a per water basis it is quite similar for both ions.

Solvent–Solvent Structural Analysis and Energetics. The solvent–solvent structural properties in the solution are very similar to those of pure water,[9] if we take into account all the waters in the solution. The rdf's computed in this way closely resemble the pure water ones, and thus we do not report these in detail.

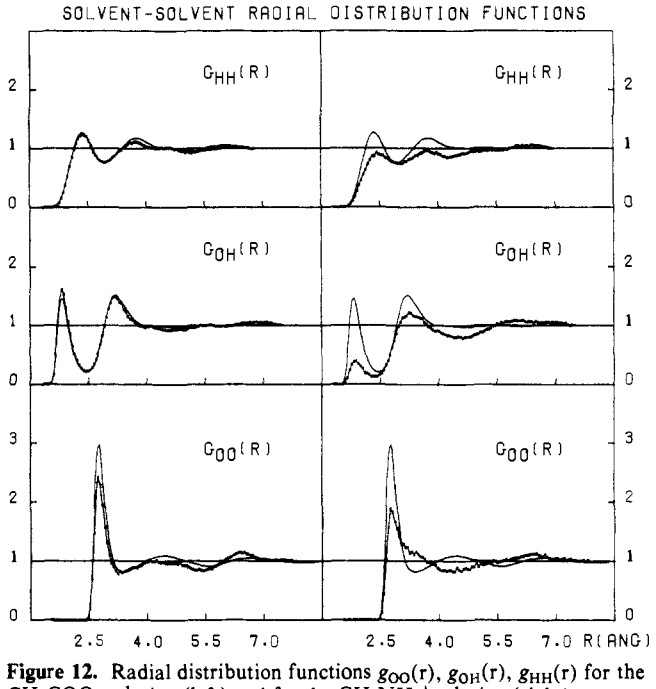

Figure 12. Radial distribution functions $g_{OO}(r)$, $g_{OH}(r)$, $g_{HH}(r)$ for the CH_3COO^- solution (left) and for the $CH_3NH_3^+$ solution (right), as seen by the waters in the polar shell.

To better illustrate the behavior of the various kinds of waters, we have recorded separately the water′–water distribution, where water′ stands for polar-shell waters, methyl-shell waters, and bulk waters. When water′ = bulk, the rdf's are essentially identical with the pure water ones, which are used for comparison below.

In Figure 12, the radial distribution functions $g_{OO}(r)$, $g_{OH}(r)$, and $g_{HH}(r)$ are compared with those of pure water, for the waters belonging to the polar shell around acetate and methylammonium, respectively. As far as the polar $O^{\delta-}$ environment is concerned, the water oxygens find less O's at nearly 2.8 Å than in pure water, because one of their coordination valences is saturated by the solute. Interestingly, the water oxygen becomes a stronger acceptor of an H bond, giving rise to a higher first peak in the g_{OH} than in pure water. This may arise because the second-shell waters are oriented by the ion and, in the process, are aligned to H bond to the polar waters.

In the methylammonium solution, the waters in the polar $H^{\delta+}$ environment have both lone pairs directed toward the solute. Hence only their hydrogens are available for coordinating to bulk water, leading to a coordination number of just half the value in bulk solution. This fact affects all three distributions in a similar manner.

The radial distribution functions around the waters belonging to the CH_3 environment, displayed in Figure 13, are more similar to the pure water ones for the acetate solution. For the methylammonium solution, the radial distribution functions are rather different, even though the basic features are conserved. The

(11) Aue, D. H.; Webb, H. M.; Bowers, M. T. *J. Am. Chem. Soc.* **1976**, *98*, 31.
(12) Millero, F. J. *Chem. Rev.* **1971**, *71*, 147.

Table IV. H Bond Analysis[a]

	bulk		shell		CH_3		polar	
	X^-	X^+	X^-	X^+	X^-	X^+	X^-	X^+
av no. of H bonds	3.13	3.16	2.76	2.45	3.10	2.74	2.42	1.88
av coord. number	5.15	5.23	4.57	4.76	4.75	4.80	4.39	4.70
S-S bonding energy	-19.57	-19.70	-14.54	-13.35	-18.42	-16.27	-10.66	-7.72
$E_{\text{H bonds}}$[b]	-4.37	-4.36	-4.35	-4.29	-4.39	-4.32	-4.31	-4.23
E_{Coulomb}	-5.79	-5.78	-5.74	-5.64	-5.74	-5.66	-5.75	-5.57
$E_{L\text{-}J}$	1.41	1.42	1.39	1.35	1.35	1.35	1.44	1.33
ϑ, deg[c]	159.4	159.3	159.8	159.3	159.6	159.6	160.2	158.5
Φ, deg[d]	100.2	99.7	100.1	102.4	99.7	102.9	100.5	101.1
			% Monomers in H-Bonds					
$N = 0$	0.2	0.2	0.6	2.0	0.3	0.9	0.8	4.2
$N = 1$	3.5	3.4	7.4	14.8	3.8	8.0	10.9	28.0
$N = 2$	18.8	18.3	29.4	33.9	19.7	28.5	39.1	44.3
$N = 3$	41.2	40.1	42.6	35.6	41.4	42.4	43.8	22.5
$N = 4$	33.7	34.6	18.5	13.1	31.7	19.4	5.3	1.0
$N = 5$	2.5	3.3	1.5	0.6	3.1	0.9	0.0	0.0

[a] Energies are in kcal/mol. [b] Total H bond energies, which have been decomposed into electrostatic (E_{Coulomb}) and Lennard-Jones ($E_{L\text{-}J}$) terms. [c] H bond angle O-H···O. [d] H bond angle H-O···H.

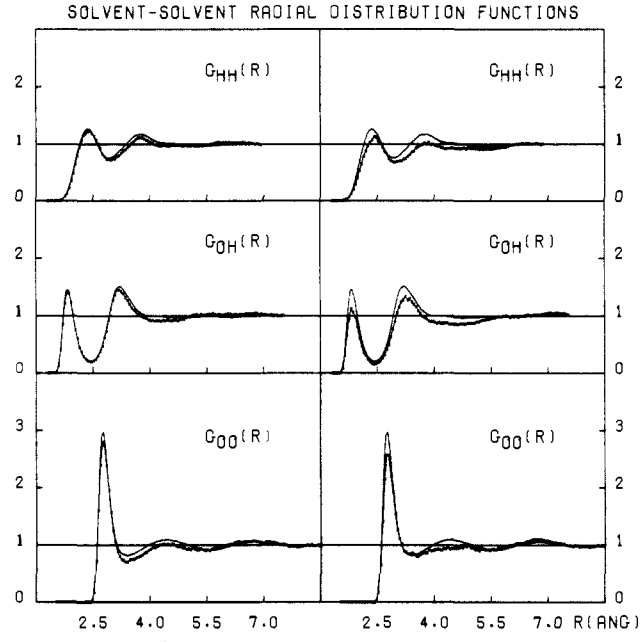

Figure 13. Radial distribution functions $g_{OO}(r)$, $g_{OH}(r)$, $g_{HH}(r)$ for the CH_3COO^- solution (left) and for the $CH_3NH_3^+$ solution (right), as seen by the waters in the methyl-group shell.

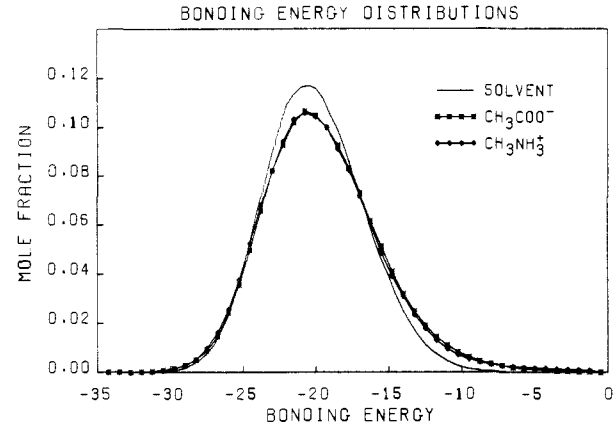

Figure 14. Bonding energy distributions for pure TIP4P water, CH_3COO^-, and $CH_3NH_3^+$. Units in ordinate are mole fraction/kcal/mol.

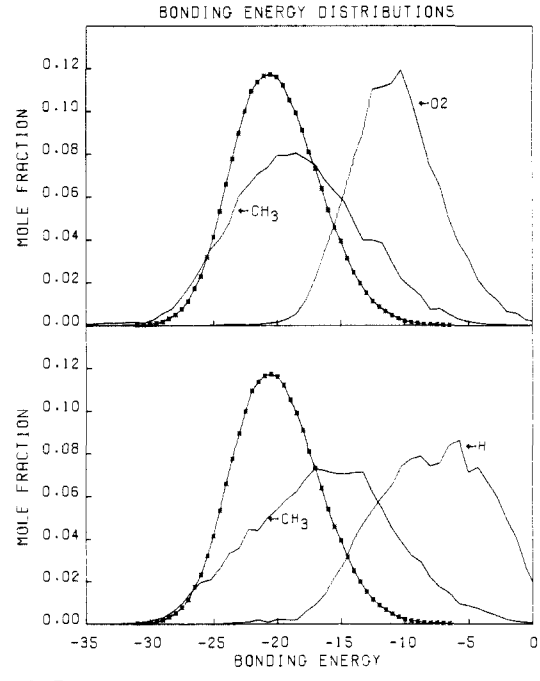

Figure 15. Bonding energy distributions as seen by the waters in the CH_3 and O2 environment for the CH_3COO^- solution (upper) and by the waters in the CH_3 and H environment for the $CH_3NH_3^+$ solution (lower), with respect to pure water.

reasons for this difference can be ascribed to the charge on the methylammonium CH_3 group, which causes the waters to have a certain Coulombic interaction with the solute also in this region.

Figure 14 contains the bonding energy distributions in both solutions in comparison with pure water. The two solutions behave in a quite similar way. The polar solute–solvent interaction leads to a higher percentage of less attractive interactions compared to pure water. The "hydrophobic effect" of the methyl groups leads to a slightly larger number of more attractive water–water interactions.[7]

To further examine this, we have decomposed the bonding energy distributions, according to the positions the waters hold around the solute (Figure 15; upper part for acetate and lower part for methylammonium solution, respectively), of the interaction energies between the first-shell waters and the water molecules enclosed within a radius of 3.5 Å around them. It can be clearly seen that the waters surrounding the methyl groups interact, at least in part, better than the molecules in pure water interact with the neighboring water molecules. The interaction is better around the CH_3COO^- methyl group that, bearing a charge lower in absolute value than the $CH_3NH_3^+$ one, shows a greater apolar character. On the other hand, the $CH_3NH_3^+$ methyl group has an intermediate behavior, still shifted toward apolar behavior, notwithstanding its high charge. The energy distribution for the waters in the polar regions again underscores that these waters

have less total attractive interactions with the other water molecules, due to the strong orienting effect of the polar solute.

Table IV contains an analysis of hydrogen bonding in the solution, using the same definition of H bonding ($E_{pair} < -2.75$ kcal/mol) used previously.[5]

Considering the bulk waters as a reference point, we notice a sharp decrease in the average number of H bonds in the shell and in the global coordination number. Also, the solvent–solvent interaction energies are less exothermic compared to pure solvent, as a consequence of the interaction with the solute. The first three entries of the table for the polar- and methyl-group regions around the solute show that the average number of H bonds is nearly as high as in pure water around the acetate methyl group, but it is less for the methylammonium methyl group. Also, the solvent–solvent bonding energy is much closer to the pure water value for the waters around the acetate methyl than the methylammonium methyl.

On the other hand, we find a sharp decrease both in the average number of H bonds and in the solvent–solvent bonding energy when we examine the polar zones; this lowering is more pronounced when we consider the methylammonium polar environment, which produces a greater disruption in the solvent.

Analogous information can be derived by examining the percentage of monomers involved in N hydrogen bonds. In fact, about 30% of the monomers are involved in four hydrogen bonds in the bulk solution and around the CH_3COO^- methyl group. This percentage is reduced by nearly one-third around the $CH_3NH_3^+$ methyl group and is statistically insignificant for the waters around the polar H's. In this region we also find that just one-half as many monomers as for pure water are involved in three H bonds, with a consequent sharp increase in the percentage forming two H bonds. In contrast, the O2 polar environment is less dramatically affected, the waters just showing the almost complete loss of the ability to form the fourth H bond with the solvent.

Discussion and Conclusions

We have presented Monte Carlo simulations on the solvation of methylammonium and acetate ions in aqueous solution. The enthalpies of solvation are calculated to be in reasonable agreement with experiment, with the calculated value 10 kcal/mol smaller than experiment for $CH_3NH_3^+$ and 9 kcal/mol smaller than experiment for CH_3COO^-. The difference in observed solvation energy between acetate and methylammonium (the anion solvation energy is ~ -14 kcal/mol more exothermic than the cation) is thus very well reproduced, even though the solvation energies are calculated to be more endothermic than experiment.

Chandrasekhar et al.[13] studied the solvation of Li^+, Na^+, Cl^-, and F^- in a box of 125 water molecules using Monte Carlo methods and found that the solvation energies of the anions were well predicted, but the exothermicities for the cations were overestimated. Carrying out the same simulations with 216 water molecules makes all the solvation energies more exothermic by 10–15%. It is thus likely that our calculated solvation energies would become more negative on going from 216 water molecules to a much larger box. However, what is encouraging here is the fact that the calculated *relative* solvation energies of anion CH_3COO^- and cation $CH_3NH_3^+$ are in satisfactory agreement with experiment, something that was not found comparing[13] the similar size ions Na^+ and F^-, where the calculated difference in solvation energy was −15 kcal/mol (Na^+ more exothermic) and the experimental difference is +14 kcal/mol (favoring F^-). Our results thus encourage studies of solvation enthalpies of larger and more complex ions.

One referee expressed a concern that the simulation presented here was not converged and might be trapped in a local minimum. In the research for a viable strategy to achieve faster convergence, we ran another MC simulation on CH_3COO^- with a different starting configuration and obtained nearly the same results,[14] thus supporting the convergence of the computed results.

Our calculated partial molar volumes are in good agreement with experiment, but there are statistical uncertainties inherent in calculating partial molar volumes by this approach.

The results of more detailed structural and energetic analysis have allowed us to more precisely understand the nature of aqueous solvation in these molecules. Although there is some ambiguity in the definition of first shells and solvation zones in nonspherical molecules, our analysis has used the geometric representation described in Figure 1 and has found a description of solvation structure that is clear and makes physical sense. Acetate has ~6 tightly bound waters around the COO^- group (as in the POO^- group in DMP), and its CH_3 group behaves as a normal nonpolar methyl as in DMP, with the cos θ distributions for those CH_3 groups very similar. H_2O does not like to turn its lone pairs or its H's toward these methyl groups.

The solvation structure around $CH_3NH_3^+$ is noticeably different. Its NH_3^+ group has an average coordination number of 3.5, corresponding to one water closely associating with each H and some fraction of a bridging water between them. However, water···CH_3 *attractions* now play a significant role in the nature of $CH_3NH_3^+$ solvation, as illustrated by the cos θ distribution for the water···CH_3 interactions there (with the water lone pair(s) pointing toward CH_3) and the many other detailed analyses reported here. This result may seem surprising at first, but not when one realizes that the "redistribution" of cationic charge near protonated amines attached to methyl groups have been known for some time. In fact in $N(CH_3)_4^+$,[16,17] the full +1 charge is likely smeared out over the H atoms. Thus, a CH_3 group attached to a protonated N would be expected to behave quite differently than a neutral hydrocarbon CH_3 or one attached to an anion. As shown clearly in Table IV, waters near the CH_3 group of $CH_3NH_3^+$ behave significantly more like the waters around the polar groups than those around the CH_3 group of CH_3COO^-, where the water behavior is quite close to that of bulk water. Although one could quibble about our choice of partial charges of the various atoms (they were least-squares fit to 6-31G* electrostatic potentials around the molecules), the use of Mulliken populations also shows a large difference between the acetate methyl and the methylammonium one. Thus, we have here an interesting exception to the idea of "transferability" of hydration properties among similar functional groups. This transferability works rather well for the acetate methyl, that in DMP, the COO^- in acetate, and POO^- in DMP. Nonetheless, the methyl groups in protonated amines appear different than "normal" CH_3 groups because of their large partial positive charge.

Acknowledgment. This work has been supported by the Italian CNR and NIH Grant GM-29072 to P.A.K. We are very grateful to Prof. W. Jorgensen for helpful comments and the data in ref 19.

Registry No. CH_3COO^-, 71-50-1; $CH_3NH_3^+$, 17000-00-9; water, 7732-18-5.

(13) Chandrasekhar, J.; Spellmeyer, D. C.; Jorgensen, W. L. *J. Am. Chem. Soc.* **1984**, *106*, 903.

(14) Alagona, G.; Ghio, C., unpublished results.
(15) Port, G. N. J.; Pullman, A. *Theor. Chim. Acta* **1973**, *31*, 231.
(16) Pullman, A.; Armbruster, A. M. *Int. J. Quantum Chem.* **1974**, *8S*, 169.
(17) Singh, U. C.; Kollman, P. *J. Comput. Chem.* **1984**, *5*, 129.
(18) Jorgensen, W. L.; Ibrahim, M. *J. Am. Chem. Soc.* **1981**, *103*, 3976.
(19) Jorgensen, W. L., private communication.